Hindawi Publishing Corporation
Shock and Vibration
Volume 2015, Article ID 817281, 12 pages
http://dx.doi.org/10.1155/2015/817281

Research Article

A Multiscale Finite Element Model Validation Method of Composite Cable-Stayed Bridge Based on Structural Health Monitoring System

Rumian Zhong, Zhouhong Zong, Qiqi Liu, and Haifei Zhou

School of Civil Engineering, Southeast University, Nanjing 210096, China

Correspondence should be addressed to Zhouhong Zong; zongzh@seu.edu.cn

Received 17 October 2014; Accepted 16 January 2015

Academic Editor: Tony Murmu

A two-step response surface method for multiscale finite element model (FEM) updating and validation is presented with respect to Guanhe Bridge, a composite cable-stayed bridge in the National Highway number G15, in China. Firstly, the state equations of both multiscale and single-scale FEM are established based on the basic equation in structural dynamic mechanics to update the multiscale coupling parameters and structural parameters. Secondly, based on the measured data from the structural health monitoring (SHM) system, a Monte Carlo simulation is employed to analyze the uncertainty quantification and transmission, where the uncertainties of the multiscale FEM and measured data were considered. The results indicate that the relative errors between the calculated and measured frequencies are less than 2%, and the overlap ratio indexes of each modal frequency are larger than 80% without the average absolute value of relative errors. These demonstrate that the proposed method can be applied to validate the multiscale FEM, and the validated FEM can reflect the current conditions of the real bridge; thus it can be used as the basis for bridge health monitoring, damage prognosis (DP), and safety prognosis (SP).

1. Introduction

With the development of traffic enterprise, many SHM systems have been implemented on cable-stayed bridge throughout the world; the importance of their damage detection and prognosis ability based on model has been recognized by highway administrations; thus, the efficiency and accuracy of the FEM have a significant impact on the structural safety assessment [1–6].

Multiscale modeling in physics is aimed at calculating system behavior on one level using information or models from different levels, since the superiority of multiscale modeling has been the focus of many investigations and discussions in recent years. For example, Oberkampf and Roy [7] and Weng et al. [8] discussed the substructural method for multiscale modeling. Liu et al. [9] described the application of bridging scale method to the coupled atomistic/continuum simulation of dynamic fracture, where the robustness of the multiscale method was demonstrated through many benchmark problems and application examples. Takizawa and Tezduyar [10] presented a multiscale space-time technique for fluid-structure interaction (FSI) computations; a number of test computations show the performance of the method. Efendiev and Hou [11] gave a brief overview of global couplings of multiscale basis functions and performed comparisons of multiscale finite volume method, mixed multiscale finite element method, and variation multiscale methods. Ben Dhia [12, 13] offered an Arlequin method to glue two models, which allows the coexistence of incompatible models, sharing the energies of the system in the superposition regions and each part can be linked in an appropriate way in the gluing subregions. However, most of the previous studies concentrated on the laws of conservation of force, mass, and energy; it is difficult to confirm lots of coupling parameters based on these equilibrium equations in civil engineering, the efficiency and accuracy of the multiscale FEM cannot be achieved at the same time.

Although several of multiscale evaluation indexes based on Runyang Bridge [14], Sutong Bridge [15], and Donghai Bridge [16] had been established, there are still a few challenges in testing accuracy of the multiscale FEM. Oberkampf

and Roy [7] provided a comprehensive and systematic development of the basic concepts, principles, and procedures for verification and validation (V&V) of models and simulations. Doebling et al. [17] and George [18] discussed the response surface method; it has been applied to a wide range of applications in industry, environmental regulations and safety, product and plant safety, financial investing, and governmental regulations. Guo and Zhang [19] combined the response surface method with Monte Carlo simulation, and a thin plate experiment was used to verify the method. Zong et al. [20, 21] completed FEM updating and validation method based on the response surface for a PC continuous rigid frame bridge. However, there have been very few studies specialized in multiscale FEM updating and validation for a composite cable-stayed bridge.

This paper presents a two-step response surface method for multiscale FEM updating and validation, and the organization is as follows. Section 2 is devoted to the theoretical formulations of the two-step response surface method, and the framework was presented; the SHM system of a composite cable-stayed bridge is introduced in Section 3; in Section 4, the multiscale FEM coupling parameters and structural parameters are updated, respectively. Based on the measured data of SHM system and the updated multiscale FEM, the uncertainties of both the model and test are discussed, and the updated model accuracy is assessed in Section 5.

2. Theoretical Formulations

2.1. A Two-Step Multiscale Model Updating Method. The method presented here is an extension and modification of the work done by Bauman et al. [22]. The motion equation of a viscously damped system subjected to a force can be written as

$$[M]\{\ddot{u}\} + [C]\{\dot{u}\} + [K]\{u\} = \{F\}. \tag{1}$$

According to the Arlequin vision, we consider that A is divided into two overlapping models A_1 and A_2. E denotes the gluing zone supposed to be a nonzero measured subset as $E = A_1 \cap A_2$ (see Figure 1).

To rebuild the model A, the weight parameter functions α and β are required to distribute energy in the gluing zone E, and they satisfy the following equalities:

$$\begin{aligned} \alpha + \beta = 1, &\quad \text{In } E, \\ \alpha = \beta = 1, &\quad \text{In } A \cap \overline{E}. \end{aligned} \tag{2}$$

Stiffness matrix K_s can be used to couple the two overlapping models A_1 and A_2; the static equilibrium equations for each modal can be shown as

$$\begin{aligned} \begin{bmatrix} \alpha K & K_{s_1}^T \\ K_{s_1} & 0 \end{bmatrix} \cdot \begin{bmatrix} \mu_1 \\ \varepsilon \end{bmatrix} = \begin{bmatrix} F_1 \\ F_0 \end{bmatrix}, \\ \begin{bmatrix} \beta K & -K_{c2}^T \\ -K_{c2} & 0 \end{bmatrix} \cdot \begin{bmatrix} \mu_2 \\ \varepsilon \end{bmatrix} = \begin{bmatrix} F_2 \\ -F_0 \end{bmatrix}, \end{aligned} \tag{3}$$

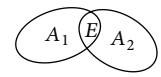

Figure 1: Superposed domains and the gluing zone E.

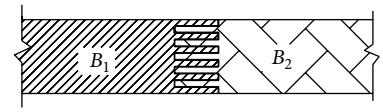

Figure 2: Graphical representation of a single-scale beam model.

where the vectors μ_1, μ_2, F_1, and F_2 stand for node displacements and loads, respectively; vector ε is a Lagrange multiplier which is related to the stiffness matrix K_s. The discrete problems in (3) are equivalent to an overall balance equation as below which can be solved based on a mixed Arlequin formulation [22]

$$\begin{bmatrix} \alpha K & 0 & K_{c1}^T \\ 0 & \beta K & -K_{c2}^T \\ K_{c1} & -K_{c2} & 0 \end{bmatrix} \cdot \begin{bmatrix} \mu_1 \\ \mu_2 \\ \varepsilon \end{bmatrix} = \begin{bmatrix} F_1 \\ F_2 \\ 0 \end{bmatrix}. \tag{4}$$

As described in the literatures [12, 13], the calculation method of the stiffness matrix K_s and the weight parameter functions α and β, which have been previously proposed, is tedious and can be affected by many factors; it determines the difficulty of applying this method to civil engineering.

The traditional multiscale modeling which is based on static equilibrium equation has been the focus of many investigations and discussion in recent years. Thus, civil engineers can now contemplate simulating complex systems spanning a large range of scales based on the dynamic equilibrium equation and two-step response surface method [21].

By virtue of (4), (1) is rewritten as

$$\begin{aligned} &\begin{bmatrix} \alpha K & 0 & K_{c1}^T \\ 0 & \beta K & -K_{c2}^T \\ K_{c1} & -K_{c2} & 0 \end{bmatrix} \cdot \begin{bmatrix} \mu_1 \\ \mu_2 \\ \varepsilon \end{bmatrix} + \begin{bmatrix} \alpha C & 0 & 0 \\ 0 & \beta C & 0 \\ 0 & 0 & 0 \end{bmatrix} \cdot \begin{bmatrix} \dot{\mu}_1 \\ \dot{\mu}_2 \\ \dot{\varepsilon} \end{bmatrix} \\ &\quad + \begin{bmatrix} \alpha M & 0 & 0 \\ 0 & \beta M & 0 \\ 0 & 0 & 0 \end{bmatrix} \cdot \begin{bmatrix} \ddot{\mu}_1 \\ \ddot{\mu}_2 \\ \ddot{\varepsilon} \end{bmatrix} = \begin{bmatrix} F_1 \\ F_2 \\ 0 \end{bmatrix}, \end{aligned} \tag{5}$$

where $[M]$, $[C]$, and $[K]$ are the mass, damping, and stiffness matrices, respectively.

For a single-scale model, we assume that a beam is divided into two overlapping models B_1 and B_2. As shown in Figure 2, the gluing zone is divided in half, and the two overlapping models B_1 and B_2 are coupled by the coupling matrix K_{s0}.

According to (5), the dynamic equilibrium equation of a single-scale model can be written as

$$\begin{bmatrix} \alpha_0 K_0 & 0 & K_{c0}^T \\ 0 & \beta_0 K_0 & -K_{c0}^T \\ K_{c0} & -K_{c0} & 0 \end{bmatrix} \cdot \begin{bmatrix} \mu_1 \\ \mu_2 \\ \varepsilon \end{bmatrix} + \begin{bmatrix} \alpha_0 C_0 & 0 & 0 \\ 0 & \beta_0 C_0 & 0 \\ 0 & 0 & 0 \end{bmatrix} \cdot \begin{bmatrix} \dot{\mu}_1 \\ \dot{\mu}_2 \\ \dot{\varepsilon} \end{bmatrix} + \begin{bmatrix} \alpha_0 M_0 & 0 & 0 \\ 0 & \beta_0 M_0 & 0 \\ 0 & 0 & 0 \end{bmatrix} \cdot \begin{bmatrix} \ddot{\mu}_1 \\ \ddot{\mu}_2 \\ \ddot{\varepsilon} \end{bmatrix} = \begin{bmatrix} F_1 \\ F_2 \\ 0 \end{bmatrix}. \tag{6}$$

From (5) and (6), the stiffness matrix K_s and the weight parameter functions α and β are approximated based on a multiscale FEM updating method. Firstly, the error between the multiscale FEM and the three-dimensional solid FEM is updated, which is so-called "first-step multiscale model updating"; and secondly combined with the visual inspection and ambient vibration testing, the error between the multiscale FE model and the real bridge is updated, which is so-called "second-step multiscale model parameters updating."

2.2. The Framework of Multiscale Model Validation. Firstly, the coupling matrix K_s and the weight parameters α and β were updated based on a two-step multiscale model updating method; moreover, considering the uncertainty of the model and test, such as the parameter error, shape error, discretization error and the uncertainty of the environment, and measured data, these parameters were all assumed to obey normal distribution. Then the parameters of uncertainty quantization and transmission were discussed based on Monte Carlo stochastic finite element method. Finally, the method was applied to a composite cable-stayed bridge; the procedure of multiscale FEM validation based on SHM system is shown as Figure 3.

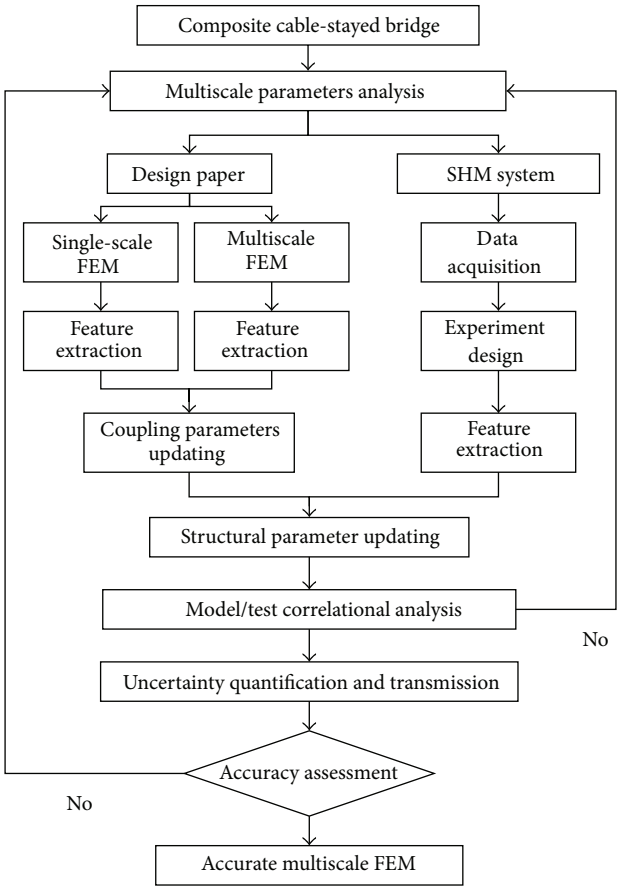

Figure 3: The multiscale FEM validation procedure based on SHM system.

3. Structural Health Monitoring System

The Guanhe Bridge is a composite cable-stayed bridge in the National Highway number G15 in China, with an overall length of 640 m and a main span of 340 m (as shown in Figure 4). The concrete bridge tower, consisting of one transverse beam, is 121 m high and was constructed using sliding formwork technology. The main girder was assembled from 166 steel I-beam segments; the bridge deck is a prestressed concrete with 34 m wide and 3.08 m high. The construction of the bridge began in 2002 and was open to traffic in May, 2006.

A comprehensive structural monitoring system (Figure 5) has been implemented on the Guanhe Bridge [23], and it comprises 280 sensors of different types, including temperature, anemometers, accelerometers, weigh-in-motion sensors, global positioning systems (GPS), displacement transducers, strain gauges, and CCTV (closed circuit television) video cameras. Such structural monitoring system has been continuously monitoring the environment conditions (e.g., wind, temperature, and traffic loads) and bridge response since 2013.

Figure 4: Guanhe Bridge panorama photo.

4. Multiscale FEM Updating

4.1. FEM of the Guanhe Bridge. The single-scale FEM and multiscale FEM were developed on the basis of the engineering drawings and implemented using the ANSYS software package. As shown in Figure 6, the cables were modeled using linear elastic link elements (LINK 8), secondary dead load was approximated as a mass element (MASS21), and the restriction effect of the rubber supports was simulated using linear elastic spring elements (COMBIN 14). For the single-scale FEM, both the bridge towers and the bridge deck were modeled using a 3D solid element (SOLID 45), and the main girder and small girder were modeled using 3D shell

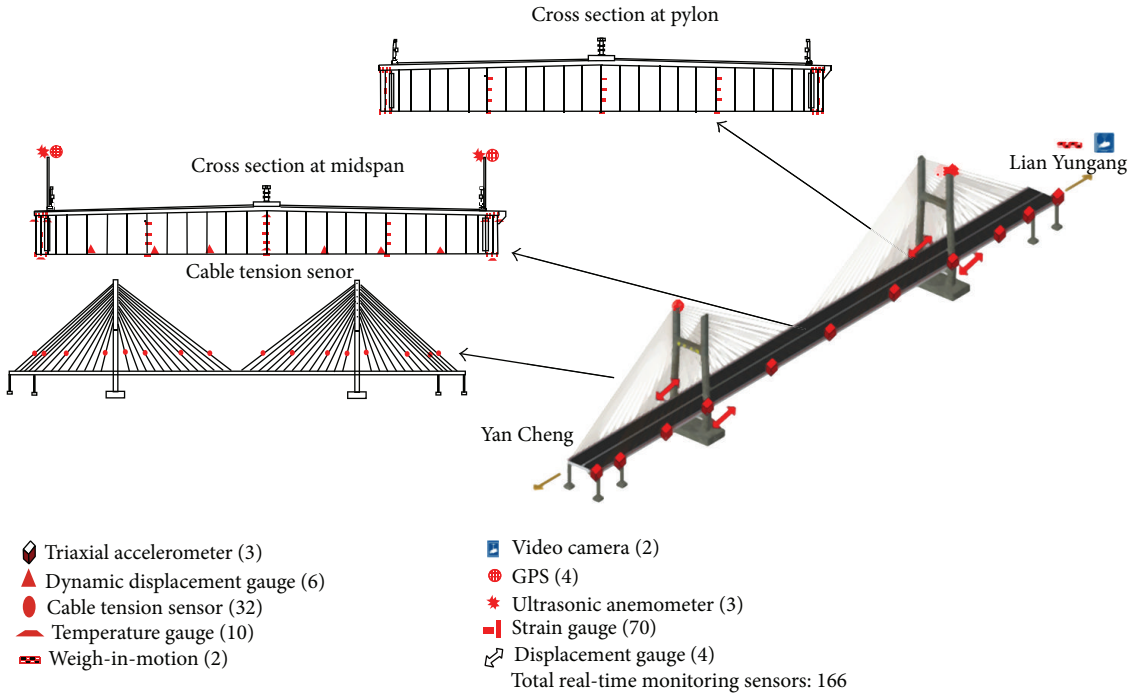

Figure 5: Sensors setting of SHM system.

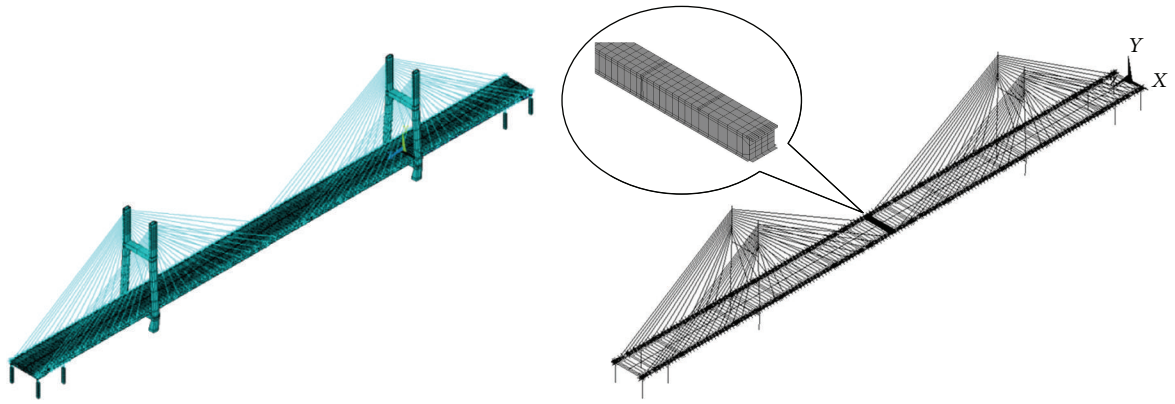

(a) The single-scale FEM (b) The multiscale FEM

Figure 6: The multiscale FE model of Guanhe Bridge.

elements (SHELL 43). However, for the multiscale FEM, both the bridge towers and the main girder of the large-scale element were simulated using three-dimensional beam elements (BEAM188), and the coupling elements of the two submodels in gluing zone E were modeled using linear elastic spring elements (COMBIN 14). The single-scale FEM and multiscale FEM, respectively, consists of 46228 and 2253 elements, respectively.

4.2. Multiscale Model Coupling Parameters Updating

4.2.1. Parameters Selection. As shown in Table 1, the weight parameters α ($\beta = 1 - \alpha$) and the coupling parameters k_v, k_t, and k_l which are related to coupling matrix K_s were selected as the independent variables; the trial results of the multiscale model show that the mode shapes and these independent variables have a close relationship, especially in the gluing

Table 1: Parameters selection.

Parameters			
k_v	k_t	k_l	α
The vertical stiffness of spring elements in the gluing zone	The transverse stiffness of spring elements in the gluing zone	The longitudinal stiffness of spring elements in the gluing zone	The weight parameter functions in the gluing zone

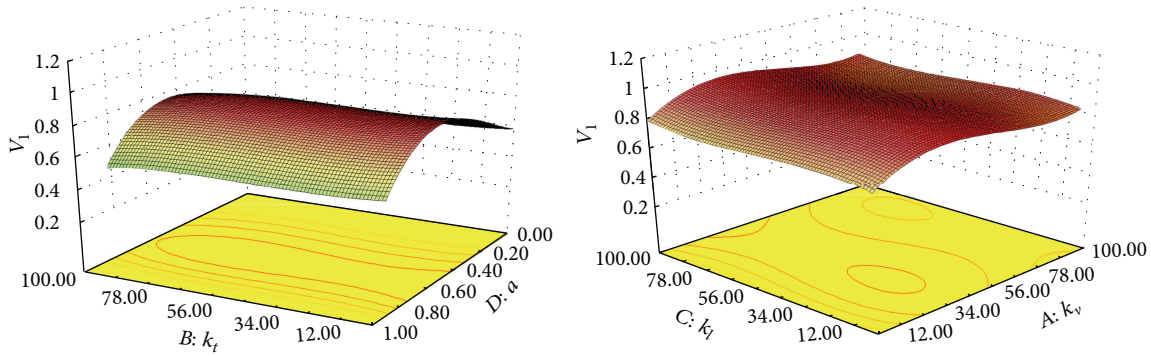

Figure 7: The response surface model of first vertical mode shape.

Table 2: Experimental samples.

N	Input variables				MAC		
	$k_v(10^7)$	$k_t(10^7)$	$k_l(10^7)$	α	V_1	T_1	L_1
1	1.00	1.00	100.00	0.57	0.72	0.98	0.84
2	79.71	43.57	22.86	0.57	0.66	0.78	0.76
3	100.00	68.25	100.00	0.69	0.93	0.32	0.89
⋮	⋮	⋮	⋮		⋮	⋮	⋮
28	76.74	1.00	1.00	0.81	0.63	0.97	0.97
29	75.25	32.19	62.88	0.81	0.64	0.63	0.75
30	1.00	26.74	73.77	0.64	0.84	0.66	0.85

Note: "N" is the number of the samples.

zone. Therefore, the model assurance criterion (MAC) values of the 1st vertical, transverse, and longitudinal mode shapes were selected as the outputs in the multiscale model updating.

4.2.2. Model Updating Based on Response Surface Method. The 3rd order response surface method is suited for the multiscale model updating, and the procedure is organized as follows: (1) the MAC values of each mode shape was calculated through the single-scale FEM; (2) the experimental samples were selected by D-optimal design method, whereas the MAC values of each mode shape under different experimental sample were calculated through the multiscale FEM, as shown in Table 2; (3) the least square regression analysis and 3rd order response surface method were used to fit these experimental samples. Then, the mathematical relationship between input and output variables can be obtained, and the response surface model of the first vertical mode shape is shown in Figure 7.

The value of R^2 and RMSE can be used to verify accuracy of the response surface model; they are calculated based on (7a) and (7b), and the results are shown in Table 3

$$R^2 = 1 - \frac{\sum_{j=1}^{N} \left[y_{\mathrm{RS}}(j) - y(j)\right]^2}{\sum_{j=1}^{N} \left[y(j) - \overline{y}\right]^2}, \tag{7a}$$

$$\mathrm{RMSE} = \frac{1}{N \cdot \overline{y}} \cdot \sqrt{\sum \left(y(j) - y_{\mathrm{RS}}(j)\right)^2}, \tag{7b}$$

Table 3: R^2 and RMSE values.

Mode	1st vertical model shape	1st transverse model shape	1st longitudinal model shape
R^2	0.9996	0.9998	0.999997
RMSE	8.78×10^{-6}	3.11×10^{-6}	5.25×10^{-7}

Table 4: The updated parameters and MAC value.

Parameters	Initial values	Updated values	MAC (%)		
			V_1	T_1	L_1
$k_v(10^7$ N/m)	1	91.32			
$k_t(10^7$ N/m)	1	2.13			
$k_l(10^7$ N/m)	1	1.59	93.51	97.11	95.43
α	0.5	0.71			
β	0.5	0.29			

where $y_{\mathrm{RS}}(j)$ is the calculated value by response surface model; $y(j)$ is the relative calculated result by finite element analysis of the multiscale model; $\overline{y}$ is the mean value by finite element analysis of the multiscale model. Table 3 shows that the values of R^2 are close to 1, and the values of RMSE are near zero. Therefore, the response surface model can show the mathematical relationship between input and output parameters. In other words, it can be used for multiscale model updating.

The parameters can be updated based on the response surface model which has been built and the updated MAC values can also be calculated. In general, it is generally acceptable when the MAC is greater than 80% [21]. The MAC values in this study are listed in Table 4: the lowest MAC is 93.51% which implies an excellent match between the mode shapes from the two methods. Therefore, it can be concluded that the mode shapes of the multiscale FEM are consistent with the single-scale FEM, and the weight parameter functions α ($\beta = 1 - \alpha$) and the coupling parameters k_v, k_t, and k_l are well suited to the multiscale model.

(a) (b)

Figure 8: Ambient vibration testing of Guanhe Bridge.

Table 5: Parameters selection.

Parameters			
K_1	K_2	K_3	E_1
The longitudinal stiffness of spring elements	The transverse stiffness of spring elements on the bridge tower	The transverse stiffness of spring elements on the bridge pier	Elasticity modulus of the concrete bridge deck

4.3. Structural Parameter Updating

4.3.1. Ambient Vibration Testing. Excitation by ambient vibration sources (i.e., passages of vehicles and trains) is conveniently utilized as input to the structure. To obtain the natural frequencies and mode shapes, 56 measure points and a reference point were arranged as shown in Figure 8, and the reference sensor was placed on the middle of the bridge. Data was sampled at 200 Hz, and each setup for all tests was recorded for duration of 15 minutes; the frequencies and mode shapes were obtained based on peak picking (PP) and stochastic subspace identification (SSI) method.

4.3.2. Parameters Selection. There are no visual cracks by means of the visual inspection of Guanhe Bridge; therefore the elasticity modulus of the concrete bridge deck and spring stiffness of the rubber supports were selected as the input parameters, as shown in Table 5.

4.3.3. Model Updating Based on Response Surface Method. In the previous section, the response surface method has been introduced. Table 6 and Figure 9 have shown experimental samples and response surface model for the model parameter updating, respectively. The value of R^2 and RMSE can also be calculated based on (8), as shown in Table 7.

Table 7 shows that the R^2 value is near to 1, and the RMSE value is near zero. Therefore, the response surface model can show the mathematical relationship between input and output parameters, so that it can be used to the multiscale model parameters updating.

Based on the response surface model, the input parameters can be updated, and the updated frequencies and MAC values of the main bridge can be calculated, as shown in Tables 8 and 9. It can be observed that the calculated frequencies from the updated multiscale FEM based on the two-step response surface method are in good agreement with the measurements, as the maximum error is not larger than 8% and the values of MAC are over 90%.

5. Multiscale FEM Validation of Guanhe Bridge

5.1. Sample Data. A total of 720 sample data were measured under the temperature of 30~35°C for the purpose of keeping ambient temperatures constant, data were sampled at 50 Hz, and all tests were recorded for duration of 30 minutes. The frequencies can be obtained based on SSI method; and the measured frequencies are assumed to obey the normal distributions based on a descriptive statistical analysis, as shown in Tables 10 and 11.

5.2. Uncertainty Analysis. A probability statistics method was used for the uncertainty quantification and transmission of the multiscale model parameters. To study the influence of structural parameters on the frequencies, we considered these three cases.

Case 1. Study on the influence of parameter N ($N = E_1/3.45 \times 10^{10}$) to the vertical frequencies, while keeping parameters K_1, K_2, and K_3 constant.

Case 2. Study on the influence of parameters K_2 and K_3 to the transverse frequencies, while keeping the others constant.

Case 3. Study on the influence of parameter K_1 to the longitudinal frequencies, while keeping the others constant.

When doing probability/statistics-based uncertainty quantification and transmission, probability distributions of the parameters should be known. However, in this study we know only the measured frequencies but not the probability distributions of the parameters. For this reason, the authors used the combination of response surface model and optimization theory. The statistical characteristics of the parameters

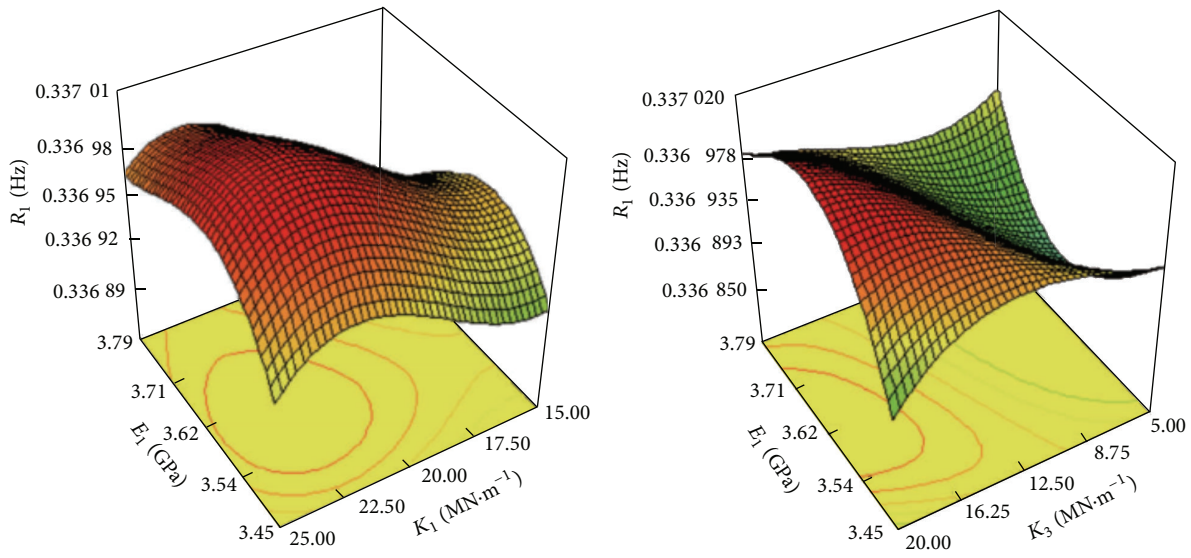

(a) The response surface model of first vertical mode shape

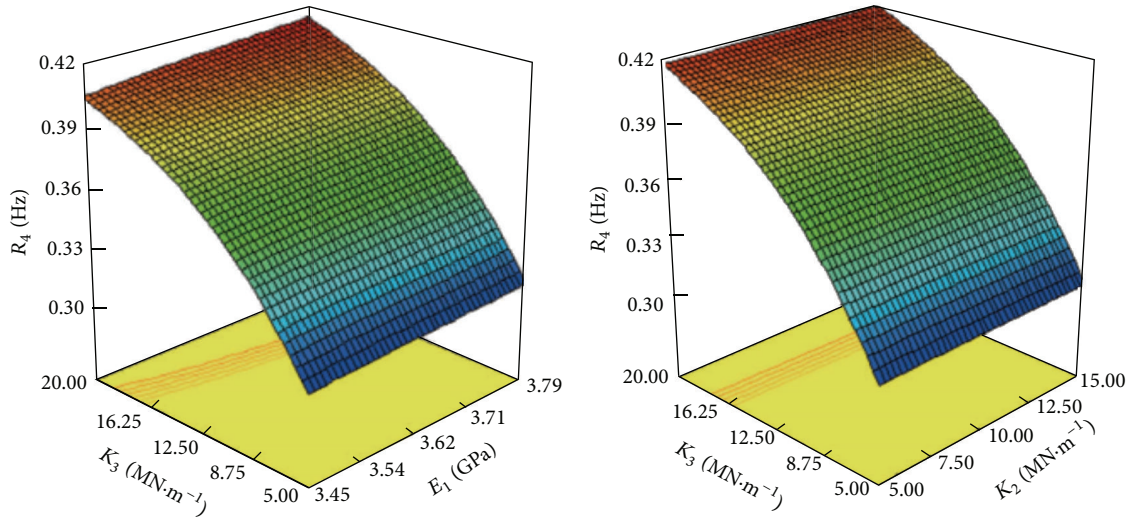

(b) The response surface model of first transverse mode shape

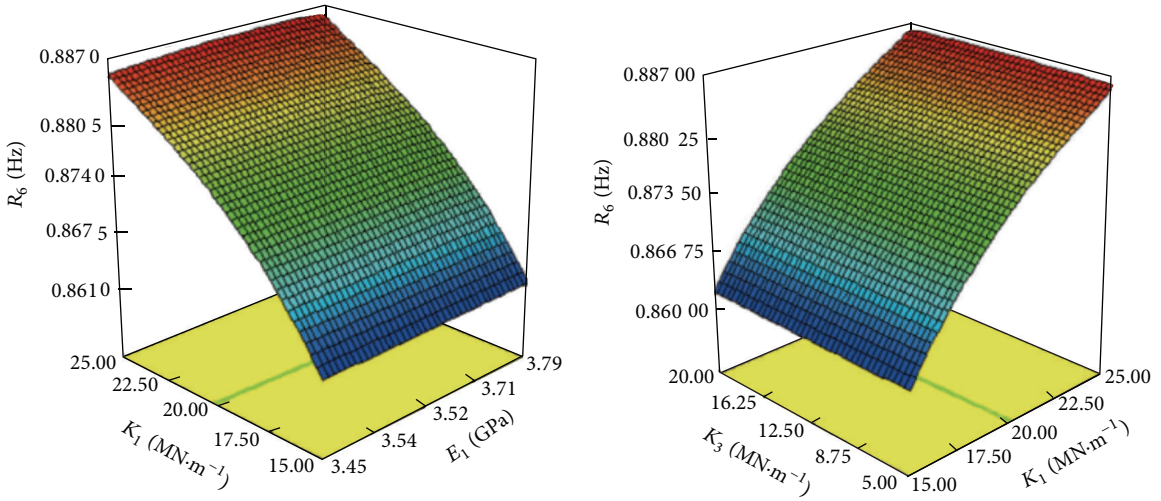

(c) The response surface model of first longitudinal mode shape

Figure 9: The response surface model of mode shape.

Table 6: Experimental samples.

N	Input parameters				Frequencies						
	A	B	C	D	R_1	R_2	R_3	R_4	R_5	R_6	R_7
1	3.45	20.71	15.00	12.08	0.347	0.505	0.797	0.377	0.531	0.878	0.585
2	3.57	25.00	5.00	18.42	0.355	0.508	0.797	0.411	0.615	0.886	0.585
3	3.80	19.37	5.00	5.00	0.362	0.512	0.799	0.311	0.423	0.875	0.585
⋮	⋮	⋮	⋮	⋮	⋮	⋮	⋮	⋮	⋮	⋮	⋮
43	3.80	17.22	15.00	8.98	0.361	0.512	0.799	0.360	0.492	0.869	0.585
44	3.80	15.00	5.00	20.00	0.362	0.512	0.799	0.423	0.636	0.861	0.585
45	3.80	25.00	5.00	11.34	0.362	0.512	0.799	0.380	0.526	0.886	0.585

Note: $A, B, C,$ and D are the values of k_v, k_t, k_l, and α; R_1–R_3, R_4-R_5, R_6, and R_7 are the frequencies of 1st–3rd vertical mode, 1st-2nd transverse mode, 1st longitudinal mode, and 1st torsion mode.

Table 7: R^2 and RMSE values.

Mode	1st vertical model shape	1st transverse model shape	1st longitudinal model shape
R^2	0.99999926	0.9999989	0.99999998
RMSE	1.55×10^{-6}	1.96×10^{-6}	2.44×10^{-7}

Table 8: Parameters change before and after updating based on the response surface method.

Parameters	Initial values	Updated values	Error/%
$E_1(\times 10^{10}$ Pa)	3.45	3.6	4.2
$K_1(\times 10^8$ N/m)	15	17.54	14.5
$K_2(\times 10^9$ N/m)	5	6.47	22.7
$K_3(\times 10^6$ N/m)	10	10.77	7.1

were obtained by inverse transformation of the model and assumed to obey normal distributions. In the following the procedure of uncertainty quantification and transmission is outlined: (1) the updated parameters can be obtained based on two-step multiscale model updating method and used as the mean values of the structural parameters; (2) based on the sample data of the measured frequencies and optimization theory, the parameters can also be calculated, and the standard deviation of these calculated values were used as the standard deviation of the structural parameters; (3) assuming that the design parameters obey normal distributions, the random numbers which conform to the probability distributions of structural parameters can be obtained based on the Monte Carlo simulation method; then the frequencies can be calculated based on the response surface model, and the probability distributions of calculated values can be compared with the measured values, as listed in Tables 12 and 13.

It can be concluded from Table 13 that (1) the transverse and longitudinal restriction effect of the rubber supports have a great influence on the transverse and longitudinal frequencies, respectively, and the variable coefficient is more than 2%, (2) the elasticity modulus of the concrete bridge deck has a larger influence on the vertical frequencies, for the variable coefficient is between 0.9% and 2.9%, and (3) the mean value of each frequency has been less affected by the uncertainty of each parameter.

5.3. Model/Test Correlation Analysis. To analyze the correlation between model and test results, overlap ratio criterion (ORC) can be used. As shown in (8), $J(p)$ is an overlap ratio index of PDF (probability density of frequency), and it can be calculated by comparing calculated frequencies of multiscale FEM with measured frequencies of ambient vibration testing. If $J(p) = 1$, it shows that multiscale FEM is completely consistent with the bridge

$$J(p) = \mathrm{PDF}_{\mathrm{test}} \cap \mathrm{PDF}. \tag{8}$$

The overlap ratio index (Figure 10) has been calculated, as shown in Table 14, and Table 15 shows the overlap ratio index of each modal frequency without the average absolute value of relative errors between calculated and measured values. It can be concluded that the average absolute value of relative errors between calculated and measured values have an influence on the overlap ratio index, without the average absolute value of relative errors, the overlap ratio index of each modal frequencies are over 80%. Thus, the updated multiscale FEM can well represent the dynamic characteristics of Guanhe Bridge.

5.4. Model Accuracy Evaluation. Considering the uncertainty of multiscale FEM, the mean values of the calculated frequencies were obtained based on the Monte Carlo simulation and response surface method. It can be seen from Table 16 that the relative errors between the calculated and measured frequencies are less than 2% with the uncertainty factors fully considered, which indicates that the multiscale FEM can reflect current conditions of the real bridge; thus it can be used as the basis for bridge health monitoring, damage prognosis (DP), and safety prognosis (SP).

6. Conclusions

A novel method termed two-step response surface method for multiscale FEM updating and validation has been developed based on the structural health monitoring system of Guanhe Bridge in this paper. The following conclusions can be drawn from the analysis and the measurements.

(1) The calculated frequencies of the updated FEM based on the two-step response surface method are in good agreement with the measured frequencies, with

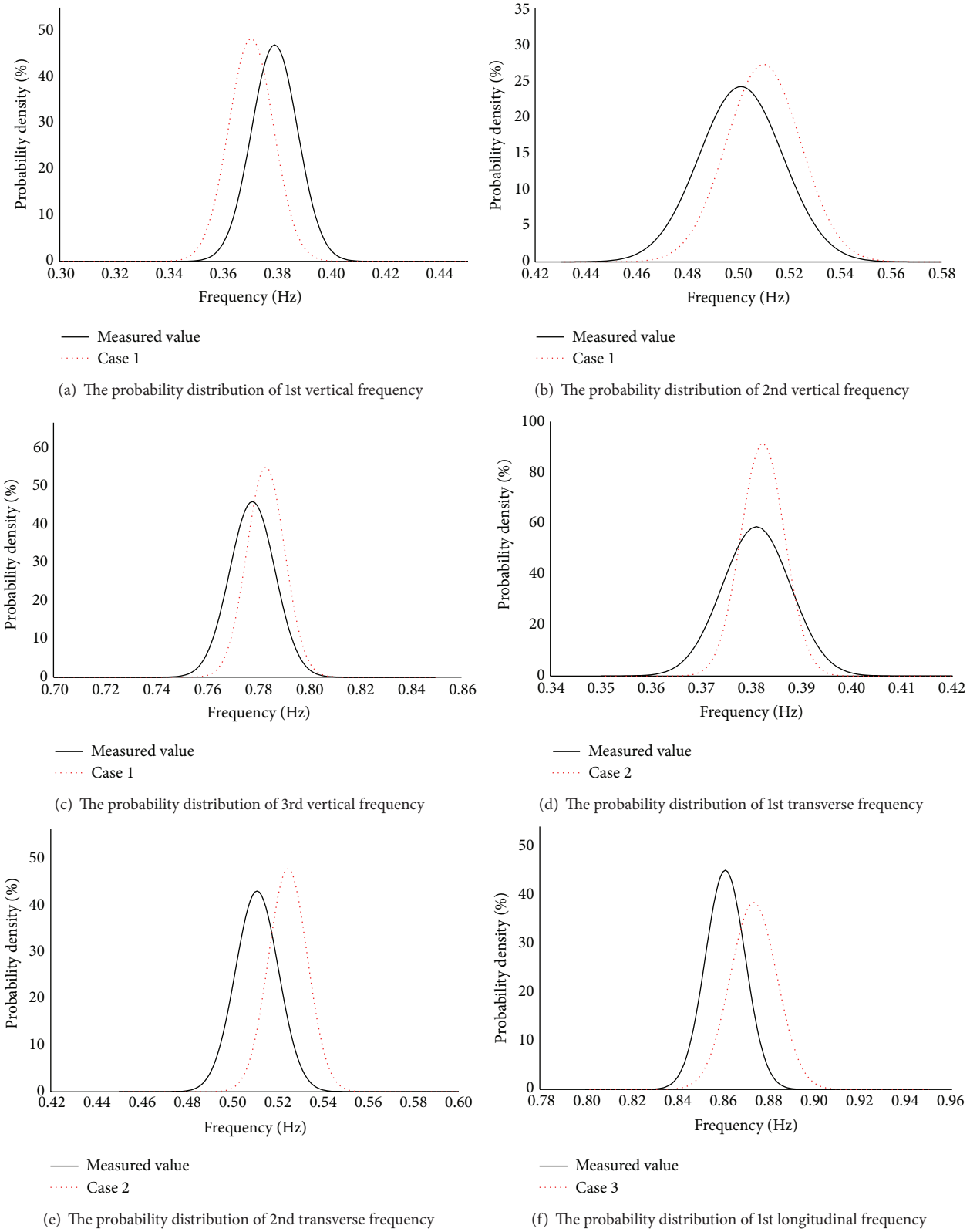

(a) The probability distribution of 1st vertical frequency

(b) The probability distribution of 2nd vertical frequency

(c) The probability distribution of 3rd vertical frequency

(d) The probability distribution of 1st transverse frequency

(e) The probability distribution of 2nd transverse frequency

(f) The probability distribution of 1st longitudinal frequency

Figure 10: The probability distribution of Guanhe Bridge frequency.

Table 9: Comparison of updated frequencies and measured frequencies, MAC values (unit: Hz).

Direction	N	Frequencies (Hz)				MAC values (%)
		Measured frequencies ①	Calculated frequencies of single-scale FEM	Updated frequencies of multiscale FEM ②	Relative error (② − ①)/① (%)	
Vertical	1	0.38	0.36	0.35	7.80	91.01
	2	0.50	0.50	0.51	2.00	91.21
	3	0.77	0.76	0.80	3.90	93.15
Transverse	1	0.39	0.28	0.37	5.13	91.11
	2	0.50	0.39	0.52	4.00	92.25
Torsion	1	0.63	0.59	0.59	6.35	92.11
Longitudinal	1	0.87	0.15	0.87	0.00	95.23

Table 10: Sample data of measured frequencies.

N	Vertical frequencies			Transverse frequencies		Longitudinal frequencies
	1	2	3	1	2	1
1	0.378	0.503	0.757	0.378	0.481	0.874
2	0.376	0.503	0.759	0.376	0.481	0.874
3	0.376	0.503	0.757	0.376	0.481	0.857
⋮	⋮	⋮	⋮	⋮	⋮	⋮
717	0.365	0.482	0.746	0.376	0.489	0.845
718	0.376	0.503	0.767	0.376	0.503	0.815
719	0.376	0.503	0.762	0.376	0.503	0.84
720	0.376	0.503	0.767	0.376	0.503	0.835

Table 11: The statistics of measured frequencies.

Model	Mean value	Standard deviation	Variable coefficient (%)
Vertical			
1st	0.379	0.0085	2.243
2nd	0.501	0.0165	3.293
3rd	0.778	0.0089	1.144
Transverse			
1st	0.381	0.0068	1.785
2nd	0.511	0.0095	1.859
Longitudinal			
1st	0.861	0.0087	1.010

the maximum error being not larger than 8% and the values of MAC being over 90%. Moreover, the updated parameters of the FEM model still keep their physical signification.

(2) The results of the multiscale FEM/test correlation analysis indicate that the overlap ratio index $J(p)$ of each modal frequency is over 80% without the average absolute value of relative errors, which means that the updated multiscale FEM can reflect well on the dynamic characteristics of Guanhe Bridge.

Table 12: Distribution characteristics of uncertainty parameters for Guanhe Bridge.

Parameters	Mean value	Standard deviation	Variable coefficient (%)	Distribution pattern
N	1.040	0.171	16.44	Normal distribution
$K_1(\times 10^8$ N/m)	17.540	0.004	0.03	Normal distribution
$K_2(\times 10^9$ N/m)	6.470	3.520	54.41	Normal distribution
$K_3(\times 10^6$ N/m)	10.770	0.484	4.49	Normal distribution

(3) Considering the influence of structural parameters uncertainties, the relative errors between the calculated and measured frequencies are less than 2%. It can be concluded that the multiscale FEM after validation can reflect well on the current conditions of the real bridge; thus it can be used as the basis for bridge health monitoring, damage prognosis (DP), and safety prognosis (SP).

Nomenclature

$[M]$: Mass matrix
$[C]$: Damping matrix
$[K]$: Stiffness matrix
$\{u\}$: Displacement vector
$\{F\}$: Force vector
α, β: Weight parameter functions
K_s: Coupling matrix
ε: A Lagrange multiplier
V_1, T_1, L_1: The MAC values of first vertical, transverse, and longitudinal mode shapes
$y_{RS}(j)$: The calculated value by response surface model
$y(j)$: The relative calculated result by finite element analysis of the multiscale model
$\overline{y}$: The mean value by finite element analysis of the multiscale model
$J(p)$: An overlap ratio index.

Table 13: The statistics of the frequencies in different conditions.

Case	Mode	Vertical frequencies			Transverse frequencies		Longitudinal frequencies
		1	2	3	1	2	1
1	Mean value (Hz)	0.37036	0.50987	0.78325	0.38117	0.52315	0.87115
	Standard deviation (Hz)	0.00825	0.01464	0.00742	0.00153	0.00452	0.00156
	Variable coefficient (%)	2.22702	2.87191	0.94695	0.40140	0.86400	0.17907
2	Mean value (Hz)	0.37012	0.50526	0.78112	0.38225	0.52465	0.87119
	Standard deviation (Hz)	0.00356	0.00421	0.00125	0.00435	0.00854	0.00985
	Variable coefficient (%)	0.96185	0.83323	0.16003	1.13748	1.62832	1.13064
3	Mean value (Hz)	0.37052	0.50891	0.78411	0.38115	0.52122	0.87335
	Standard deviation (Hz)	0.00289	0.00394	0.00156	0.00098	0.00115	0.02740
	Variable coefficient (%)	0.77998	0.77420	0.19895	0.25712	0.22064	3.13689

Table 14: Overlap ratio index of each modal frequency with the average absolute value of relative errors.

Mode	Vertical model shape			Transverse model shape		Longitudinal model shape
	1	2	3	1	2	1
$J(p)$	0.736	0.782	0.821	0.778	0.451	0.573

Table 15: Overlap ratio index of each modal frequency without the average absolute value of relative errors.

Mode	Vertical model shape			Transverse model shape		Longitudinal model shape
	1	2	3	1	2	1
$J(p)$	0.896	0.857	0.816	0.805	0.810	0.821

Table 16: Comparison of average values of each modal frequency.

Mode	Vertical frequencies			Transverse frequencies		Longitudinal frequencies
	1	2	3	1	2	1
Calculated frequency (Hz)	0.379	0.501	0.778	0.381	0.511	0.861
Measured frequency (Hz)	0.378	0.503	0.765	0.378	0.512	0.86
Relative error (%)	0.26	0.40	1.67	0.79	0.20	0.12

Disclaimer

The viewpoints of this paper represent only the authors' opinion; they do not represent the views of the fund committee.

Conflict of Interests

The authors declare that there is no conflict of interests regarding the publication of this paper.

Acknowledgment

The authors gratefully acknowledge the financial support provided by the Natural Science Foundation Committee of China (Grant no. 51178101 and no. 51378112).

References

[1] J. Ou and H. Li, "Structural health monitoring in mainland china: review and future trends," *Structural Health Monitoring*, vol. 9, no. 3, pp. 219–231, 2010.

[2] D. J. Inman, C. R. Farrar, V. L. Junior, and V. S. Junior, *Damage Prognosis for Aerospace—Civil and Mechanical Systems*, John Wiley & Sons, London, UK, 2005.

[3] M. Luczak, A. Vecchio, B. Peeters, L. Gielen, and H. van der Auweraer, "Uncertain parameter numerical model updating according to variable modal test data in application of large composite fuselage panel," *Shock and Vibration*, vol. 17, no. 4-5, pp. 445–459, 2010.

[4] Y. Lei, C. Liu, Y. Q. Jiang, and Y. K. Mao, "Substructure based structural damage detection with limited input and output measurements," *Smart Structures and Systems*, vol. 12, no. 6, pp. 619–640, 2013.

[5] H. Shahverdi, C. Mares, W. Wang, and J. E. Mottershead, "Clustering of parameter sensitivities: examples from a helicopter airframe model updating exercise," *Shock and Vibration*, vol. 16, no. 1, pp. 75–87, 2009.

[6] Y. Chandra, R. Chowdhury, F. Scarpa et al., "Vibration frequency of graphene based composites: a multiscale approach," *Materials Science and Engineering B: Solid-State Materials for Advanced Technology*, vol. 177, no. 3, pp. 303–310, 2012.

[7] W. L. Oberkampf and C. J. Roy, *Verification and Validation in Scientific Computing*, Cambridge University Press, London, UK, 2010.

[8] S. Weng, Y. Xia, Y.-L. Xu, and H.-P. Zhu, "An iterative substructuring approach to the calculation of eigensolution and eigensensitivity," *Journal of Sound and Vibration*, vol. 330, no. 14, pp. 3368–3380, 2011.

[9] W. K. Liu, D. Qian, S. Gonella, S. Li, W. Chen, and S. Chirputkar, "Multiscale methods for mechanical science of complex materials: bridging from quantum to stochastic multiresolution

continuum," *International Journal for Numerical Methods in Engineering*, vol. 83, no. 8-9, pp. 1039–1080, 2010.

[10] K. Takizawa and T. E. Tezduyar, "Multiscale space-time fluid-structure interaction techniques," *Computational Mechanics*, vol. 48, no. 3, pp. 247–267, 2011.

[11] Y. Efendiev and T. Y. Hou, *Multiscale Finite Element Methods—Theory and Applications*, Springer, London, UK, 2009.

[12] H. B. Dhia and C. Zammali, "Level-Sets and Arlequin framework for dynamic contact problems," *Revue Europeenne des Elements*, vol. 13, no. 5–7, pp. 403–414, 2004.

[13] H. Ben Dhia, "Multiscale mechanical problems: the Arlequin method," *Comptes Rendus de l'Académie des Sciences—Series IIB: Mechanics-Physics-Astronomy*, vol. 326, no. 12, pp. 899–904, 1998.

[14] Y. Ding, A. Li, D. Du, and T. Liu, "Multi-scale damage analysis for a steel box girder of a long-span cable-stayed bridge," *Structure and Infrastructure Engineering*, vol. 6, no. 6, pp. 725–739, 2010.

[15] S. Chen, Z. Chen, and W. Wang, "Multi-scale detection techniques for local scour monitoring in river bed: case study at Sutong bridge," in *Earth and Space*, pp. 2431–2441, 2010.

[16] W. Zhang, C. S. Cai, and F. Pan, "Finite element modeling of bridges with equivalent orthotropic material method for multi-scale dynamic loads," *Engineering Structures*, vol. 54, pp. 82–93, 2013.

[17] S. W. Doebling, F. M. Hemez, J. F. Schultze, and A. L. Cundy, "A metamodel-based approach to model validation for nonlinear finite element simulations," in *Proceedings of 20th International Modal Analysis Conference (IMAC '02)*, pp. 671–678, February 2002.

[18] P. George, *Response Surface Method*, VDM Publishing, Saarbrücken, Germany, 2008.

[19] Q. Guo and L. Zhang, "Finite element model validation in structural dynamics," *Chinese Journal of Applied Mechanics*, vol. 22, no. 4, pp. 572–578, 2005 (Chinese).

[20] Z. Zong and W. Ren, *Finite Element Model Updating and Model Validation of Bridge Structures*, China Communications Press, Beijing, China, 2012, (Chinese).

[21] R. Zhong, X. Fan, X. Huang, and Z. Zong, "Multi-scale finite element model updating of composite cable-stayed bridge based on two-phase response surface methods," *Journal of Southeast University*, vol. 43, no. 5, pp. 993–999, 2013 (Chinese).

[22] P. T. Bauman, H. B. Dhia, N. Elkhodja, J. T. Oden, and S. Prudhomme, "On the application of the Arlequin method to the coupling of particle and continuum models," *Computational Mechanics*, vol. 42, no. 4, pp. 511–530, 2008.

[23] Z. H. Zong, X. C. Fan, and R. M. Zhong, "A study on the design of health monitoring system for Guanhe River Bridge," in *Proceedings of the 6th World Conference Control and Structural Monitoring*, Barcelona, Spain, 2014.